Optik 124 (2013) 6840–6845

Contents lists available at ScienceDirect

Optik

journal homepage: www.elsevier.de/ijleo

A novel method of camera pose estimation by parabolic motion

Wei Liu [a], Wenxiao Shi [a,*], Yaowen Lv [b,c], Jingtai Cao [b], Yumei Yin [b], Yuanhao Wu [b], Jihong Wang [a], Xuefen Chi [a]

[a] College of Communication Engineering, Jilin University, 5372 Nanhu Road, Changchun 130012, China
[b] Changchun Institute of Optics, Fine Mechanics and Physics, Chinese Academy of Sciences, 3888 Nanhu Road, Changchun 130033, China
[c] Graduate School of Chinese Academy of Sciences, Beijing 100039, China

ARTICLE INFO

Article history:
Received 9 January 2013
Accepted 23 May 2013

Keywords:
Computer vision
Pose estimation
Parabolic motion
Projective geometry

ABSTRACT

Camera pose estimation is a basic and crucial problem in computer vision, accordingly a novel method is proposed for pose estimation based on parabolic motion in our paper. Firstly, the intersection of lines which are the image plane projection of free-falling trajectories in different locations is computed. According to the properties of vanishing point, the intersection is defined as the vanishing point in gravity direction. Secondly, the image plane projected curve of parabolic trajectory is obtained by Sampson Approximation. Finally, the camera pose is estimated by employing the projective geometry properties of vanishing point and vanishing line implicated in the projected parabola, provided that the intrinsic parameters of camera are specified. The absolute Euclidean distance of translation is obtained innovatively with the known frame frequency. Numerical simulation as well as practical experiment in this paper demonstrates the correctness and feasibility of our method, with the known frame frequency, as the experiment show that compared with the traditional checkerboard method the mean errors of rotation axis, rotation angle and translation are respectively 0.017 rad, 0.007 rad and 11.650 mm by our method. It can generally satisfy the accuracy requirements of camera.

1. Introduction

Camera pose estimation, *i.e.* the location of camera is to determine its pose and position through the image obtained by camera. Its broad application prospect includes vision navigation, robot localization, target identification, photogrammetry, *etc.* [1–4]. In the past thirty years, this problem has been lucubrated, thus giving birth to many methods.

For now, the methods of camera pose estimation are mainly divided into two categories: pose estimation with the intrinsic parameters of camera specified, and pose estimation with the intrinsic parameters of camera unspecified. Camera intrinsic parameters calculation, namely camera calibration, has already been solved through the endeavor of many researchers. Henceforth we assume the pose estimation mentioned in our paper to be the pose estimation of calibrated camera. Currently, researches on calibrated camera pose estimation mainly focus on two directions. One is the Perspective N Points (P*n*P) problem initiated by Fishler and Bolles [5]. P*n*P problem can be described as finding the pose of an object from the image of n points at known location on it. With the work of many scholars, P*n*P problem has gradually made its progress. The essence of P*n*P problem is how to determine the unique solution from the multiple solutions for $N < 6$, under the existing constraint condition [6–11]. The other is to estimate camera pose by employing the geometric restrictions of scene such as coplanar, parallel and orthogonal properties to estimate the camera pose. Typical research has been done by Hartley and Zisserman [12], where they apply squares and orthogonal parallels in estimating camera pose. In addition, circles and parallels are used in camera pose estimation in [13–17].

The above methods require the feature point position of objects or the special relationship of geometric construction to be known. Due to the effect of earth gravity, any thrown objects shall obey the law of parabolic motion. After familiarizing ourselves with the projective geometry properties, we propose a novel method to estimate camera pose. Firstly, we assume the object to be in free falling motion in different locations. By extracting the image plane projection of free falling motion, we successfully obtain the vanishing point in gravity direction. Then we can obtain the vanishing lines of the supporting plane of parabola by the projective geometry properties implicated in the parabola, and finally extract the camera pose information from vanishing points and vanishing lines, including rotation axis, rotation angle and translation. In this paper, we innovatively obtain the absolute Euclidean distance of translation with the known frame frequency. Due to its no requirement for information of objects or geometric elements in the scene, this

* Corresponding author. Tel.: +86 431 85152811; fax: +86 431 85152811.
E-mail address: swx@jlu.edu.cn (W. Shi).

0030-4026/$ – see front matter © 2013 Elsevier GmbH. All rights reserved.
http://dx.doi.org/10.1016/j.ijleo.2013.05.074

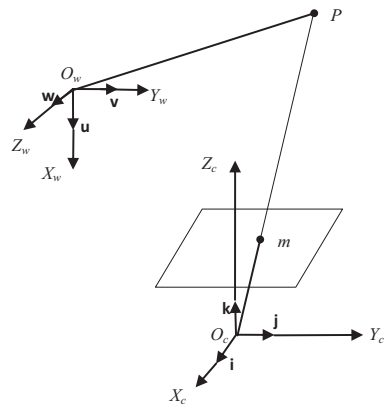

Fig. 1. The pinhole camera model.

method is rather feasible. Meanwhile, this method needs only a section of the parabolic trajectories, thus enabling the pose measurement of multiple cameras.

The structure of our paper is arranged as follow: the second part introduces the theoretical background knowledge of the pose estimation method in our paper. The third part gives the detailed algorithm of pose estimation. The forth part lists the results of the synthetic data simulation of our method. The fifth part applies our algorithm in estimating binocular measurement system and compares it with the traditional checkerboard method. Eventually, in the sixth part, we summarized the whole paper.

2. Background knowledge

2.1. Camera model

The classical pinhole camera model is shown in Fig. 1 [18,19]. $O_c - X_cY_cZ_c$ is the coordinate system of camera, O_c is the optical center of camera, the coordinate axes O_cX_c and O_cY_c are respectively parallel to the rows and columns of the image plane, O_cZ_c is the optical axis of camera.

The unit vectors of three coordinate axes are respectively: **i**, **j**, **k**. $O_w - X_wY_wZ_w$ is the built World Coordinate System (WCS), **u**, **v**, **w** are the unit vectors of the coordinate axes of WCS. If the translation vector from WCS to the camera coordinate system is **t**, the rotation matrix is **R**. **t** is the representation of the origin O_w of WCS in camera coordinate system, then the rotation matrix **R** can be expressed as:

$$\mathbf{R} = \begin{bmatrix} u_i & v_i & w_i \\ u_j & v_j & w_j \\ u_k & v_k & w_k \end{bmatrix} = \begin{bmatrix} {}^c\mathbf{u} & {}^c\mathbf{v} & {}^c\mathbf{w} \end{bmatrix} \tag{1}$$

where, ${}^c\mathbf{u}$, ${}^c\mathbf{v}$, ${}^c\mathbf{w}$ are respectively the coordinate representations of the unit vectors of WCS coordinate axes in camera coordinate system [20,21].

In this model, any point P in the space and its projection m on camera image plane satisfy the projection formula below:

$$\mathbf{s}\begin{bmatrix} u \\ v \\ 1 \end{bmatrix} = \mathbf{K}[\mathbf{R}\cdot\mathbf{t}]\begin{bmatrix} x \\ y \\ z \\ 1 \end{bmatrix} \tag{2}$$

where (u, v) is the image coordinate of projective point m, (x,y,z) is the three-dimensional coordinate of P in WCS, **K** is the matrix of camera intrinsic parameters, **R**, **t** are respectively the rotation matrix and translation vector from WCS to camera coordinate system.

2.2. Results by the calibrated camera

(1) On the image plane of camera, a point m gives a straight line through the optical center of camera. The direction of ray **d** under the measurement in the camera coordinate system is [12]:

$$\mathbf{d} = \mathbf{K}^{-1}\mathbf{m} \tag{3}$$

where **m** is the coordinate of point m.

(2) A straight line l on the image plane as well as the optical center of camera determines a plane in the space, to which the direction of normal line **n** in the camera coordinate system is [12]:

$$\mathbf{n} = \mathbf{K}^T\mathbf{l} \tag{4}$$

where **l** is the equation of the line l.

2.3. The projective geometry of parabola

The properties of vanishing point and vanishing line are widely applied in the self-calibration of camera [22]. The camera plane projection of an infinite point on the straight line is the vanishing point of the line. In fact, all parallel lines and the plane at infinity intersect at the same infinite point. Therefore, parallel lines have the same vanishing point, which is only determined by the direction of lines and unaffected by the position of lines. The image plane projections of the parallel lines intersect at the same point, *i.e.* the vanishing point in the direction of parallel lines. According to Eq. (3), provided that the intrinsic parameters of camera are known, the direction of straight line can be determined by the vanishing point.

In three-dimensional space, parallel planes and the plane at infinite intersect at a common straight line, the image of the straight line is called the vanishing line of the plane.

Vanishing line, nonrelated to the position of scene plane, only depends on the normal direction of the scene plane. According to Eq. (3), provided that the intrinsic parameters of camera are known, the direction of straight line can be determined by the vanishing point.

According to the properties of vanishing point and vanishing line, with the inherent characteristics of the projective geometry of the parabola, we have the following conclusions:

(1) The projective curves of parabolas on the image plane have a mutual intersection, namely the vanishing point in the earth gravity direction.
(2) At the mutual intersection of the projective curves of parabolas, the tangent is the vanishing line of the supporting plane of the parabola.

Proof. Establish a coordinate system on the supporting plane of parabola as below: set any point on the parabola as the origin, and the direction of earth gravity as the direction of x-axis, the direction normal to x-direction is defined as y-direction, as shown in Fig. 2.

We first consider the parabola on the supporting plane 1, and then the projective geometry of the parabola can be expressed as:

$$\begin{bmatrix} x & y & t \end{bmatrix}\begin{bmatrix} 0 & 0 & d \\ 0 & b & e \\ d & e & 0 \end{bmatrix}\begin{bmatrix} x \\ y \\ t \end{bmatrix} = 0 \tag{5}$$

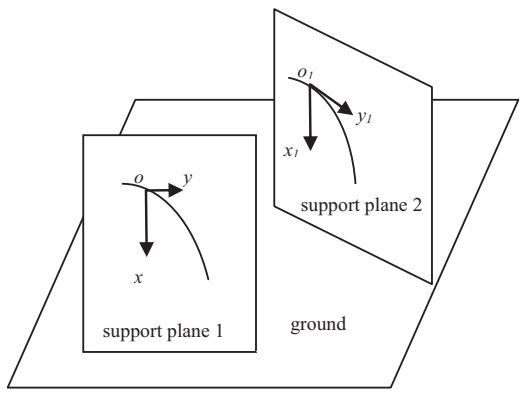

Fig. 2. The parabolic geometry.

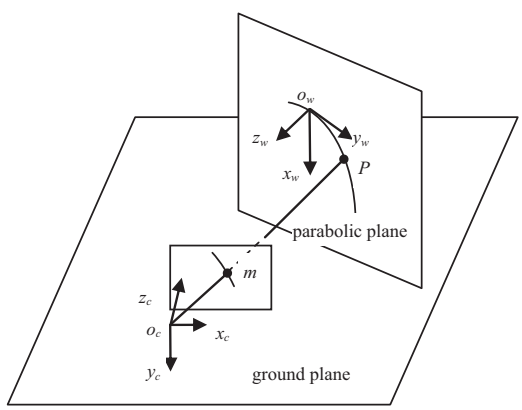

Fig. 3. The model of pose estimation.

Obviously, an infinite point $P(1,0,0)$ is on this parabola, to which the tangent at point P is:

$$\mathbf{l} = \begin{bmatrix} 0 & 0 & d \\ 0 & b & e \\ d & e & 0 \end{bmatrix} \begin{bmatrix} 1 \\ 0 \\ 0 \end{bmatrix} = \begin{bmatrix} 0 \\ 0 \\ d \end{bmatrix} \tag{6}$$

where $\mathbf{l}$ is a line at infinity on the plane. Since projection transformation can sustain the relationship of pole and polar, the projective curve on the camera plane of the parabola must pass through the projection of point P, namely $P1$. The tangent to the projective curve at point $P1$ is the vanishing line of the supporting plane.

It is clear that $P1$ is the vanishing point of straight line ox. Similarly, the tangent to the projective curve at point $P1$ is the vanishing line of the supporting plane. Hence we derive that $ox||o_1x_1$ and $P1$ and $P2$ coincide with each other in that both ox and o_1x_1 are the earth gravity direction. Since we adopt two random parabolas herein, the conclusion (1) and (2) are proved.

3. Camera pose estimation

3.1. Solving the rotation vector

In camera pose estimation, the WCS takes an arbitrary point O_w on the parabola as the origin, the earth gravity direction is the direction of x_w axis, plane $o_w - x_wy_w$ is the supporting plane where the parabola is located, y_w axis takes the moving direction of the parabola as the positive direction. The direction of the z_w axis in WCS can be determined by the right-hand coordinate system. As to determining the coordinate system of camera, it is similar to that of the pinhole camera model in Fig. 1. The model of camera pose estimation is shown in Fig. 3.

We shall divide rotation vector $\mathbf{R}$ between two coordinate systems into three rows, namely $(\mathbf{r}_1, \mathbf{r}_2, \mathbf{r}_3)$, then $\mathbf{r}_1$ is the 3D coordinate of $\mathbf{u}_1$ (the unit vector of gravity direction) in the camera coordinate system. By Eq. (3), once $\mathbf{u}_1$ is determined, we have:

$$\mathbf{r}_1 = \pm \frac{\mathbf{K}^{-1}\mathbf{u}_1}{norm(\mathbf{K}^{-1}\mathbf{u}_1)} \tag{7}$$

where, vanishing point $\mathbf{u}_1$ is the intersection of camera plane projection of free falling trajectories, norm represents the 2-*norm* of vector. By conclusion 2.3 combined with Eq. (4), we have:

$$\mathbf{r}_3 = \pm \frac{\mathbf{K}^T(\mathbf{C}\mathbf{u}_1)}{norm(\mathbf{K}^T(\mathbf{C}\mathbf{u}_1))} \tag{8}$$

where $\mathbf{C}$ is the matrix of camera plane projection of parabola. In practical measurement, $\mathbf{r}_1, \mathbf{r}_3$ might not be completely orthogonal, so we can reevaluate $\mathbf{r}_1, \mathbf{r}_3$ by Singular Value Decomposition (SVD). Then by the orthogonal properties of the rotation matrix, we have:

$$\mathbf{r}_2 = \mathbf{r}_3 \times \mathbf{r}_1 \tag{9}$$

Therefore we obtain four groups of solutions for $\mathbf{R}$, but only two of them can ensure that the reconstructive 3-D point is located in front of the camera. Then with the directivity of free falling, only one solution is satisfactory.

3.2. Absolute Euclidean Metric in the movement

In lack of the Absolute Euclidean Metric information of the scene, we can barely determine the direction $\mathbf{t}$ of the translation vector between two coordinate systems, namely:

$$\mathbf{t} = \frac{\mathbf{K}^{-1}\mathbf{v}_0}{norm(\mathbf{K}^{-1}\mathbf{v}_0)} \tag{10}$$

where, $\mathbf{v}_0$ is the camera plane projection of the origin o_w of WCS.

According to the reconstruction theory of planar scene, under the condition that the intrinsic parameters are known, we can fulfill the similar reconstruction of planar scene by utilizing the solution $\mathbf{R}$ and the direction $\mathbf{t}$ of translation vector. That is to say, the metric unit of the supporting plane of parabola and the Absolute Euclidean Metric differ by a constant factor. So the Absolute Euclidean distance between two points on the supporting plane of parabola is necessary to upgrade similar reconstruction to Absolute Euclidean Metric reconstruction. We hereby solve this scale factor by the Absolute Euclidean information in parabolic motion.

For objects in parabolic movement with no air resistance, the well-known dynamical equation along the x-direction is given by:

$$x_n = v_x \cdot (n \cdot \Delta t) + \frac{1}{2} g \cdot (n \cdot \Delta t)^2 \tag{11}$$

where x_n is the x-direction coordinate of the moving point at time n, Δt is the exposure time interval of camera, v_x is the x-direction component motion at the origin, g is the gravity acceleration constant, then we have:

$$x_{n+1} + x_{n-1} - 2x_n = g \cdot \Delta t^2 \tag{12}$$

The above equation described the Absolute Euclidean Metric of the supporting plane of parabola in that g, Δt are known, thus scale factor k is calculated as:

$$k = \frac{g \cdot \Delta t^2}{x'_{n+1} + x'_{n-1} - 2x'_n} \tag{13}$$

where, x'_{n+1}, x'_n, x'_{n-1} are the coordinates of x at respective times reinstated by unit translation vector. The Absolute Euclidean Metric of translation vector $\mathbf{T}$ is expressed as:

$$\mathbf{T} = k \cdot \mathbf{t} \tag{14}$$

3.3. Summary of the camera pose estimation algorithm

(1) By allowing movement of free falling in different locations, we obtain the projective straight lines L_i of free falling trajectories. Due to the measuring error, projective straight lines will not intersect at one point, we employ the below Eq. (15) to solve the intersections, and then vanishing point u_1 is known.

$$E = \min \sum_i d^2(u_1, L_i) \tag{15}$$

where $d(u_1, L_i)$ is the distance between u_1 and straight line L_i.

(2) By throwing the object, image coordinates at different times are obtained, the projective parabola C can be evaluated by Sampson Approximation. Then we solve $\boldsymbol{r}_1, \boldsymbol{r}_2, \boldsymbol{r}_3$ by Eqs. (7)–(9) and thus determine the unique solution of rotation matrix $\mathbf{R}$, based on the directivity of the reconstruction point of free falling movement and the fact the construction point is located in front of the camera.

(3) The direction $\mathbf{t}$ of the translation vector can be determined by Eq. (10). Subsequently reconstruction coordinates x'_{n+1}, x'_n, x'_{n-1} are obtained, and then translation vector $\mathbf{T}$ is derived by Eq. (14).

What might be an exception is the projection of parabola would degrade to a straight line when the supporting plane of parabola passes through the optical center of the camera, which is the vanishing line of the supporting plane. Hence, we can obtain r_3 by Eq. (4) and normalization.

4. The simulation with synthetic data

In the numerical simulation, the intrinsic parameters matrix $\mathbf{K}$ of camera is set as:

$$\mathbf{K} = \begin{bmatrix} 566 & 0 & 322 \\ 0 & 674 & 255 \\ 0 & 0 & 1 \end{bmatrix} \tag{16}$$

The distortion parameter of the camera lens is 0. Resolution is 1024×1024. The parabolic equation in WCS, the Rodrigues notation $\mathbf{R}v$ of rotation matrix from WCS to camera coordinate system, and the translation vector t are respectively:

$$\begin{aligned} &x = 5000 \times tm + 5000 \times tm^2; \\ &y = 5000 \times tm; \\ &z = 0; \\ &\mathbf{R}v = [-1.7937, -2.0695, -0.4908]; \\ &\mathbf{t} = [-158.02, -232.71, 705.91]; \end{aligned} \tag{17}$$

where tm is the movement time. If Gauss noise is increased by 0.9 pixel at projective point, the influence curve of image points on the shaft angle error is shown in Fig. 4.

If the number of projective points is 12, the influence curve of noise on shaft angle error is shown in Fig. 5.

Where, the calculation results of the rotation matrix $\mathbf{R}$ are the mean value of 100 calculation results.

Since vanishing points in the gravity direction are also on the projective curve of parabola, the projective points mentioned in our paper include the vanishing points in the gravity direction.

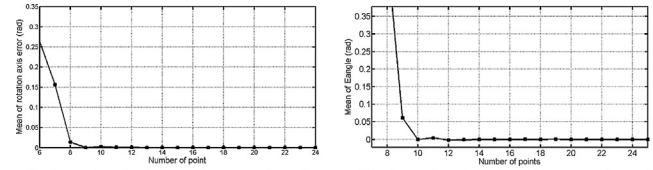

(a) The number of calculate points *vs.* rotation axis (b) The number of calculate points *vs.* rotation angle

Fig. 4. The number of calculate points *vs.* rotation axis and angle.

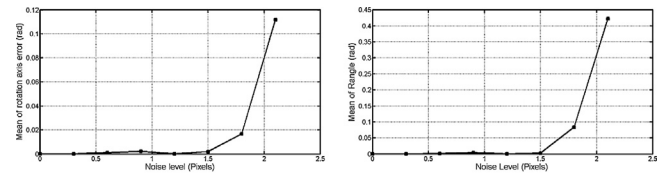

(a) The noise level *vs.* rotation axis (b) The noise level *vs.* rotation angle

Fig. 5. The noise level *vs.* rotation axis and angle.

The error of rotation axis is calculated by the shaft angle formula, namely:

$$\begin{aligned} &Eaxis = \arccos(\mathbf{n} \cdot \mathbf{n}_i) \\ &Eangle = abs(\theta - \theta_i) \end{aligned} \tag{18}$$

where *Eaxis* is the error of rotation axis, whose unit is radian (rad); *Eangle* is the error of rotation angle, whose unit is also rad. $\mathbf{n}$, θ are respectively the unit rotation axis and the rotation angle, the relationship between $\mathbf{n}$, θ and rotation vector is given by:

$$\begin{aligned} &\theta = norm(\mathbf{R}v) \\ &\mathbf{n} = \frac{\mathbf{R}v}{norm(\mathbf{R}v)} \end{aligned} \tag{19}$$

where $\mathbf{R}v$ is the Rodrigues notation of rotation matrix. From the simulation results, we can conclude:

(1) Five projective points are enough to determine the image plane projection of parabola, but we recommend adopting more than 10 projective points to reduce the calculation error in practice.

(2) The calculation error sharply increases while the noise of projective points accumulates. Thus we shall improve the measuring accuracy of projection points or increase the number of projective points.

5. Experiments with real images

Binocular vision sensor is widely used in visual measurement and three-dimensional measurement [23,24]. In our experiment, we adopt a binocular camera, whose intrinsic parameters are calibrated by Matlab toolbox. Firstly, we let the ball do six times free falling movement. By Eq. (15), the vanishing points of the two camera image planes in the gravity direction are computed.

Then we throw the ball and let the ball do parabolic motion and use the algorithm in our paper to estimate the rotation matrices $\mathbf{R}_l$ and $\mathbf{R}_r$ of left and right cameras relative to WCS of parabola. Translation vectors are $\mathbf{T}_l$ and $\mathbf{T}_r$ [25]. Then the structure parameters of binocular camera are expressed as:

$$\begin{aligned} &\mathbf{R} = \mathbf{R}_r \mathbf{R}_l^{-1} \\ &\mathbf{T} = \mathbf{T}_r - \mathbf{R}\mathbf{T}_l \end{aligned} \tag{20}$$

where $\mathbf{R}$ is the rotation matrix from right camera coordinate system to left camera coordinate system. $\mathbf{T}$ is the translation vector between two camera coordinate systems.

We repeatedly throw the ball until the sixth time and compute the structure parameters of binocular camera, followed by

Table 1
Comparison of the two methods.

Methods	Rotation vector			*Eaxis*/*Eangle* (rad)	Translation			Error (mm)
Chessboard	0.171	−0.748	−0.399	–	709.94	−117.45	203.48	–
Experiment 1	0.195	−0.753	−0.408	0.031/0.009	721.47	−119.53	206.68	12.144
Experiment 2	0.163	−0.756	−0.395	0.015/0.005	712.65	−125.84	202.20	8.906
Experiment 3	0.158	−0.748	−0.407	0.012/0.004	720.18	−112.56	201.52	11.514
Experiment 4	0.161	−0.756	−0.393	0.015/0.004	722.43	−117.03	204.83	12.570
Experiment 5	0.174	−0.740	−0.395	0.016/0.008	719.40	−114.98	206.96	10.380
Experiment 6	0.169	−0.744	−0.376	0.015/0.014	714.14	−107.30	194.19	14.385
Mean		–		0.017/0.007		–		11.650

Fig. 6. The photo of experiment.

comparing the structure parameters calculated by our method and the true value, namely the rotation matrix and translation vector determined by traditional checkerboard [26].

In our experiment, two CCD cameras (DMK31BG03.H, produced in Imaging Source) are adopted to build the experimental platform. The resolution of camera is 1024×768, pixel size is $4.65\ \mu m \times 4.65\ \mu m$, frame frequency is 60 fps, and the constructed experimental platform is shown in Fig. 6.

The images of checkerboard and parabolic ball, collected by left and right cameras when calculating structure parameters, are shown in Fig. 7.

The measured structure parameters are shown in Table 1, where the mean error of translation vector is the included angle between the parabolic calculation vector and the checkerboard calculation vector.

The experimental results show that, the structure parameters calculated by the method in our paper is approximate to that calculated by Matlab toolbox checkerboard. That is to say, our method can estimate the parameters of camera pose accurately.

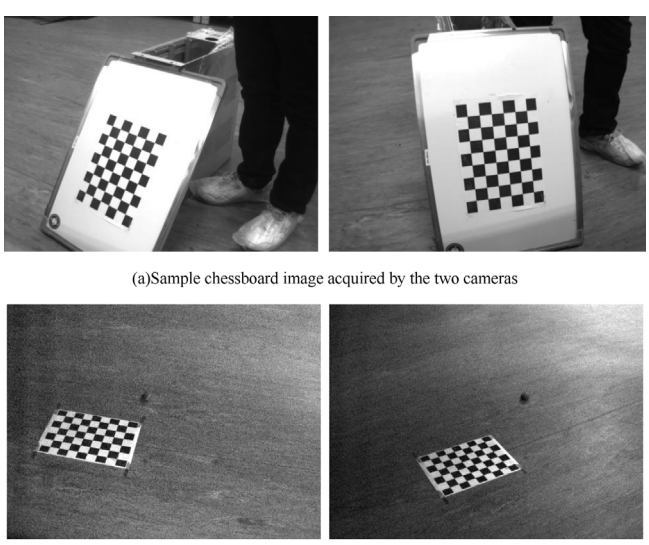

(a)Sample chessboard image acquired by the two cameras

(b)Sample parabolic ball image acquired by the two cameras

Fig. 7. Sample images acquired from the experiment.

6. Conclusion

According to the exclusive projective geometry properties of parabolic movement, in this paper we proposed a novel method based on parabolic motion to estimate the camera pose.

As we assume the intrinsic parameters of camera are specified, letting the object do free falling and parabolic movement is adequate for us to estimate camera pose is, while no structural or geometric information of the scene is necessary. Firstly, in our paper, we introduced the pinhole camera model and the important conclusion of calibrated camera, meanwhile demonstrated the properties of the vanishing point and vanishing line implicated in the parabolic motion. Secondly, we employ these properties to estimate the parameters of camera pose. And eventually, we proved the correctness and feasibility of the algorithm by simulation and the practical application in the pose estimation of binocular camera. The experimental results show that compared with the traditional checkerboard method the mean errors of rotation axis and rotation angle are 0.017 rad and 0.007 rad, respectively. With the known frame frequency, the mean errors of translation are 11.650 mm. It can generally satisfy the accuracy requirements of camera.

Acknowledgment

This work was supported by the National Natural Science Foundation of China (No. 60972028).

References

[1] L. Li, Z.-Q. Deng, B. Li, X. Wu, Fast vision-based pose estimation iterative algorithm, Optik - Int. J. Light Electron Opt. (2012), http://dx.doi.org/10.1016/j.ijleo.2012.03.018.
[2] Z. Zhang, Y. Han, Y. Zhou, M. Dai, A novel absolute localization estimation of a target with monocular vision, Optik - Int. J. Light Electron Opt. (2012), http://dx.doi.org/10.1016/j.ijleo.2012.03.032.
[3] Y. Guo, J. Wan, M. Lu, W. Niu, A parts-based method for articulated target recognition in laser radar data, Optik - Int. J. Light Electron Opt. (2012), http://dx.doi.org/10.1016/j.ijleo.2012.08.035.
[4] M. Sarkis, K. Diepole, Camera-pose estimation via projective Newton optimization on the manifold, IEEE Tans. Image Process. 21 (April (4)) (2012) 1729–1741.
[5] M.A. Fishler, R.C. Bolles, Random sample consensus: a paradigm for model fitting with applications to image analysis and automated cartography, CACM 24 (6) (1981) 381–395.
[6] X.S. Gao, J. Tang, On the probability of the number of solutions for the P4P problem, Math. Imaging Vision 25 (1) (2006) 79–86.
[7] R. Horaud, B. Conio, O. Leboulleux, B. Lacolle, An analytic solution for the perspective 4-point problem, Comput. Vis. Graphics Image Process. (47) (1989) 33–44.
[8] Z.Y. Hu, F.C. Wu, A note on the number of solutions of the noncoplanar P4P problem, IEEE Trans. Pattern Anal. Mach. Intell. 24 (4) (2002) 550–555.
[9] F.C.H. Wu, Z.H.Y. Hu, Linear method for P*n*P problem, J. Softw. 14 (3) (2003) 682–688.
[10] G.H. Wang, Z.H.Y. Hu, F.C. Wu, Single view based measurement on space planes, J. Comput. Sci. Technol. 19 (3) (2004) 831–840.
[11] L. Quan, Z. Lan, Linear n-point camera pose determination, IEEE Trans. Pattern Anal. Mach. Intell. 21 (August (8)) (1999) 774–780.

[12] R.I. Hartley, A. Zisserman, Multiple View Geometry in Computer Vision, second ed., Cambridge University Press, Cambridge, 2004.
[13] G. Wang, J. Wu, Z. Ji, Single view based pose estimation from circle or parallel lines, Pattern Recogn. Lett. (29) (2008) 977–985.
[14] A. Ansar, K. Daniilidis, Linear pose estimation from points or lines, IEEE Trans. Pattern Anal. Mach. Intell. 25 (2003) 578–589.
[15] G. Jiang, L. Quan, Detection of concentric circles for camera calibration, in: Proc. ICCV, 2005, pp. 333–340.
[16] X. Meng, H. Li, Z. Hu, A new easy camera calibration technique based on circular points, in: Proc. BMVC, 2000.
[17] J.S. Kim, P. Gurdjos, I.S. Kweon, Geometric and algebraic constraints of projected concentric circles and their applications to camera calibration, IEEE Trans. Pattern Anal. Mach. Intell. 27 (4) (2005) 637–642.
[18] B.W. Yang, L.Y. Zhang, N. Ye, et al., Camera calibration technique of wide-area vision measurement, Acta Opt. Sin. 32 (9) (2012) 0915001.
[19] Y.X. Han, Z.S. Zhang, M. Dai, Monocular vision system for distance measurement based on feature points, Opt. Precision Eng. 19 (5) (2011) 1110–1116.
[20] D.F. Dementhon, L.S. Davis, Model-based object pose in 25 lines of code, Int. J. Comput. Vis. 15 (2) (1995) 123–141.
[21] C.H.B. Xiang, D. Xie, T.H. Liu, et al., A two-step algorithm for estimating postures of cameras located in different points of view, Opt. Precision Eng. 16 (10) (2008) 1982–1986.
[22] F.C. Wu, Mathematical Methods in Computer Vision, Science Press, Beijing, 2011, pp. 77–79, 378–382.
[23] Y. Zhang, Y. Liu, Closed-form solution for circle pose estimation using binocular stereo vision, Electron. Lett. 44 (21) (2008) 1246–1247.
[24] E. Chinellato, B.J. Grzyb, A.P. del Pobil, Pose estimation through cue integration: a neuroscience-inspired approach, IEEE Trans. Syst. Man Cybernet. Pt B 42 (2) (2012) 530–538.
[25] J.J. Hou, G. Wei, J.H. Sun, Calibration method for binocular vision based on matching synthetic images of concentric circles, Acta Opt. Sin. 32 (3) (2012) 0315003–315011.
[26] Z. Zhang, Camera calibration with one-dimensional objects, IEEE Trans. Pattern Anal. Mach. Intell. 26 (7) (2004) 892–899.